 Cytometry 29:136–146 (1997)

Classification of Organelle Trajectories Using Region-Based Curve Analysis

Anna H.N. de Win,[1]* Marcel Worring,[2] Jan Derksen,[1] and Elisabeth S. Pierson[1]

[1]Department of Experimental Botany, Catholic University Nijmegen, Nijmegen, The Netherlands
[2]Department of Computer Science, WINS, University of Amsterdam, Amsterdam, The Netherlands

Received 21 October 1996; Accepted 16 May 1997

A method based on analysis of the region of movement and the functioning of the acto-myosin cytoskeleton has been elaborated to quantify and classify patterns of organelle movement in tobacco pollen tubes. The trajectory was dilated to the region of movement, which was then reduced to give a one-pixel-wide skeleton, represented by a graph structure. The longest line in this skeleton was hypothesized to represent the basic track of the organelle along a single actin filament. Quantitative features were derived from the graph structure, direction of movement on the longest skeletal line, and distance between skeletal line and particle. These features corresponded to biological events like the amount of linear movement or the probability of attachment of an organelle to the actin filament. From 81 analyzed organelle trajectories, 17 had completely linear, 17 had completely non-linear, and 47 had alternating linear and non-linear movement. Selected features were employed for classification and ranking of the movement patterns of a representative sample of the population of organelles moving in the cell tip. The presented methods can be applied to any field where analysis and classification of particle motion are intended. Cytometry 29:136–146, 1997. © 1997 Wiley-Liss, Inc.

Key terms: trajectory analysis; particle motion; organelle movement; cytoskeleton; pollen tube

Targeted movement of cells, nuclei, organelles, or intracellular substances is one of the most striking features common to biological systems. In animal cells, most types of movement are brought about by interaction between microtubules and motor molecules, i.e., kinesin or dynein (39). Organelle movement in plant cells is essentially coupled to the interaction between actin filaments and myosin molecules (33,36,42), although proteins resembling microtubule associated motor proteins have been found (1). Actin filaments are conserved structures, which consist of a rather straight and unbranched strand of actin monomers with a polarity that dictates the direction of movement (6,23,32). Single actin filaments of sometimes opposite polarity may be arranged into bundles. The use of anti-actin antibodies or specific markers for filamentous actin, like phalloidin, has revealed the presence of a dense network of actin filaments (6,18,31,35). Recent observations (17,30) indicate that bundles of actin filaments in living plant cells also have a certain flexibility. Myosin molecules are capable of translocating particles over single actin filaments by a combination of energy consumption and conformational changes of the molecule (12,26). Many myosin molecules are located on the surface of cellular organelles (8,20,44).

Pollen tubes, the long cylindrical cells through which the sperm cells move to the ovary, are favorite objects for the study of organelle movement (9,10,23,25) and the cytoskeleton (5,13,15,19,22–24,36,37). Early reports describe regular cytoplasmic streaming as a flow of the cytoplasm in distinct lanes through the tube. In lily (11) and tobacco (4), for example, the streaming pattern is from base to tip and vice-versa in the tube and reverse fountain-like behind the tip. Application of video-enhanced contrast microscopy to these cells has shown that organelles move as individual elements with regards to their velocity, direction and movement pattern (9,10,25).

Analysis of the movement patterns of organelles from different sources resulted in a preliminary classification (41) that distinguished three types of random movement, such as restricted Brownian motion, and eight types of active movement, such as continuous movement with constant or irregular velocity, saltatory movement, and interrupted movement with pauses and reversals of direction. These different types of movement suggest that organelle movement is not simply vectorial movement based on a continuous and constant interaction between microtubules or actin filaments and motor molecules.

*Correspondence to: A.H.N. de Win, Plant Cell Biology Group, Department of Experimental Botany, Catholic University Nijmegen, Toernooiveld 1, NL 6525 ED Nijmegen, The Netherlands.

Differences among movement patterns might be brought about by regulation of the motor molecules, by the morphology of the cytoskeleton, by mutual interaction between organelles (25), by physical factors like viscosity or steric hindrance, or by superimposed random movement.

Although numerous descriptions of organelle movements exist, few studies contain numeric measurement. To our knowledge, this article is the first to provide a quantitative analysis of organelle movement in a plant cell. It presents a method to classify organelle movement patterns according to non-subjective criteria. In the first step, region-based curve analysis (43) is performed on the trajectory of each organelle. In this way, a single line is obtained, which is assumed to represent the basic track of the organelle along a single actin filament. In the second step, evaluation of the trajectory, projected on this hypothetical actin filament, gives quantitative features that allow identification and characterization of different modes of movement. In the third step, these quantitative data are employed to define an ordering in classes and a continuous ranking.

MATERIALS AND METHODS

Data Collection

Pollen tubes of *Nicotiana tabacum* L. cv. Samsun were cultured in vitro (4) at 28°C for 1.5 to 2.5 h and transferred to a microscope slide. Samples were observed with an Univar microscope (Reichert-Leica, Vienna, Austria) using Nomarski differential interference contrast (DIC) optics in which organelles appeared as shadow-casted disks. Observations were done with a Plan Apo ×100 oil iris lens, NA=1.32 (Univar microscope), infinity corrected, an internal ×1.6 magnifying lens and two integrated heat filters. The optical *x*,*y*-resolution was about 0.21 µm and the depth of visibility about 0.6–0.8 µm. The movements of organelles in the median focal plane were recorded with video-enhanced contrast (VEC) techniques (16). Sequences of the video recording were converted to series of time-lapsed images with an interval of 0.40 s and a pixel size of 0.027 μm^2 (Fig. 1). These digital images were further employed to determine interactively the positions of the organelles, i.e., the centre of the organelles image, by using a Video Image and Data Analysis System (VIDAS, version 2.1, Kontron; Eching, Germany) (2). The positions were collected with an accuracy of about 0.03 µm and reflected the position in the cell. Only organelle trajectories which could be observed for at least 2.40 s were included and measured as long as they were visible in the focal plane. A total of 81 organelles were measured in the apical 18 µm of the tip of a pollen tube with a diameter of 9 µm. The diameter of the organelles (average 0.40 µm) was estimated by comparison of their image with disks of known size (2). The error of measurement in the diameter was estimated to 0.06 µm. The radius of the organelle is abbreviated to r_{org}.

Region-Based Curve Analysis

In (43) a new method for motion analysis was introduced in which the two-dimensional region where the

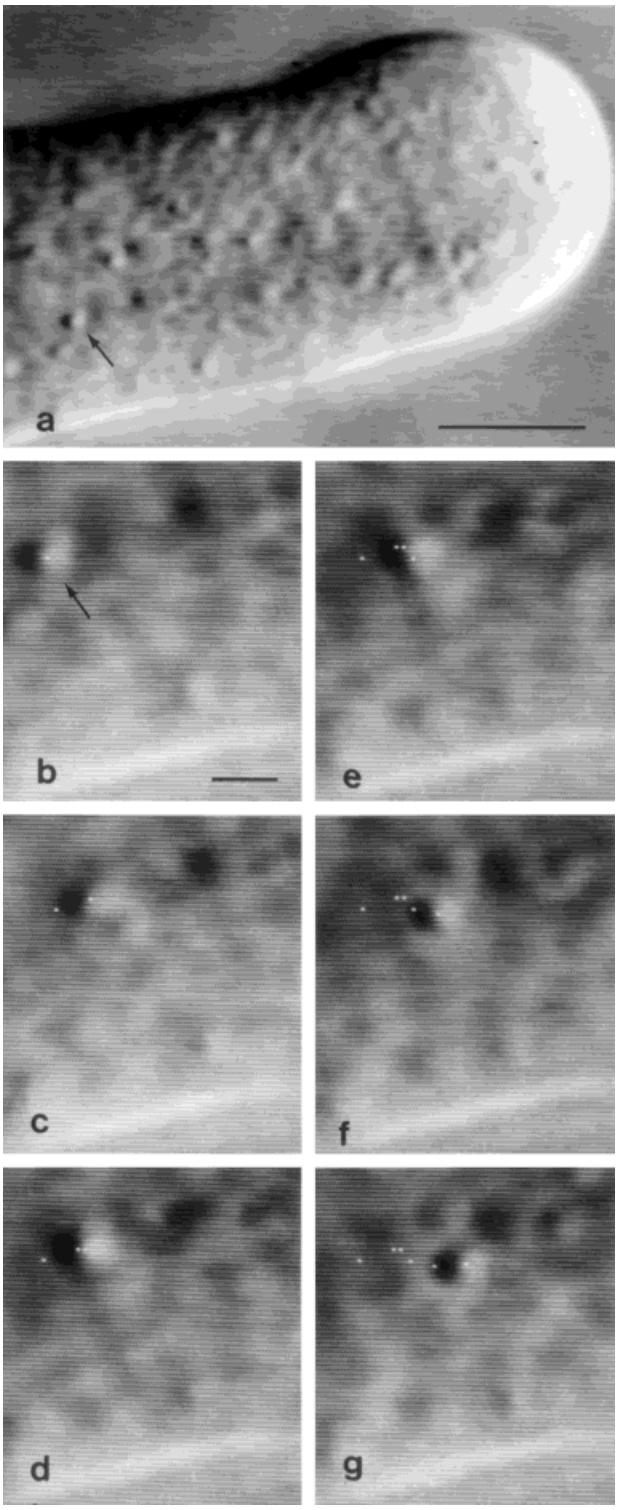

FIG. 1. Measurement of organelle movement. **a:** Overview of the tip of the pollen tube. The arrow points at the organelle that will be measured. **b–g:** Sequence at 0.40 s interval. b: The arrow points at the measured organelle of which the centre was interactively marked with the cursor. c–g: Marked positions from previous images are copied onto the current image and the new position of the centre is marked. Scale bars: a = 6 µm, b–g = 1 µm.

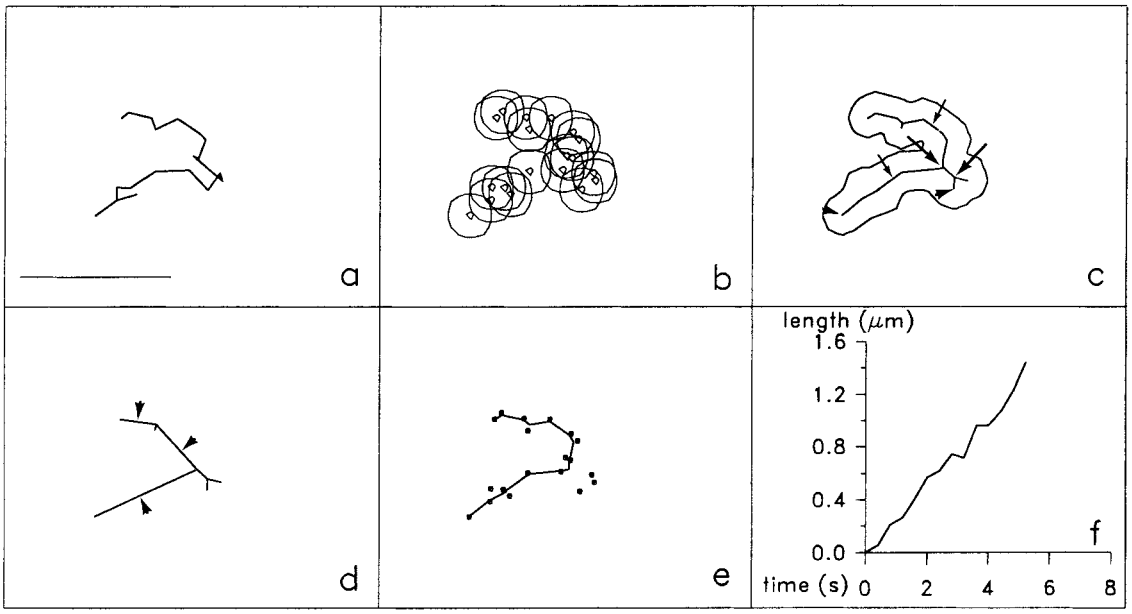

FIG. 2. Steps in the region-based curve analysis. **a:** The original trajectory is drawn as a line image. **b:** The line is dilated to a region with disks the size of the organelle radius. Some of the disks are drawn. **c:** The outline of the region is drawn. The region is reduced to give a one-pixel-wide skeletal line. Arrowhead: end point, cardinality=1; small arrow: link point, cardinality=2; large arrow: branch point, cardinality=3. **d:** The skeletal line is converted to a graph structure of the set of end and branch points in the skeleton. The path lengths of the corresponding skeletal line segment are attributed to the edges and the longest path (arrowheads) is defined. **e:** The longest skeletal line derived from the longest path (see c). The original positions (dots) are projected on this line. **f:** A time plot of the length from the start along the longest skeletal line to each projected position shows the course of the movement. Scale bar = 1 μm.

movement takes place is considered, in contrast to traditional methods that consider movement as a curve. In this paper we will elaborate on that approach by feature measurement and a classification scheme. We first briefly describe the method of region-based curve analysis performed with the SCIL_Image (Centre of Image Processing and Pattern Recognition; Delft, The Netherlands) image processing environment (38).

- Time-lapsed (x,y) data are converted into a continuous curve l by linear interpolation of the points (Fig. 2a).
- The region in which the organelle has moved is reconstructed by dilation of l with a disk with a radius equal to r_{org} (Fig. 2b). As a consequence, parts of the line closer together than the diameter of the organelle merge into a larger region. In practice, this is computed by viewing l as a two-dimensional image and placing a pixel grid on it with a grid constant significantly smaller than the distance between two observed points. A discrete distance transform is then used to compute for each grid point an approximation of the distance to l. Once this value is attained, the dilation can be computed by selecting all points with a distance smaller or equal to r_{org}. The resolution of the applied pixel grid was higher than that of the VIDAS, and the latter, therefore, determines the accuracy of the following feature measurements.
- The resulting binary image is reduced to a one-pixel-wide skeleton (Fig. 2c). Again, the discrete distance transform is used for implementation; the skeletal line is formed by connecting the points which locally have maximal distance to the boundary of the region (for more details, see 7,21). Prior to skeleton computation, holes in the binary image of the movement region were removed because they interfere with formation of a skeleton consisting of a main line with side branches. In the resulting skeletal line, three types of points can be distinguished: end points, link points, and branch points (Fig. 2c). End points have only one neighboring pixel in the skeletal line and therefore have a cardinality of 1. Link points have neighboring pixels on exactly two sides and a cardinality of 2. Branch points are connected to three or more pixels of the skeletal line and hence have a cardinality of at least 3.
- The structure of the skeleton corresponds to a graph structure where the vertices, defined by the set of end and branch points of the skeleton, are related by an edge if they are connected in the skeleton through a set of successive link points (Fig. 2d). Note that the vertices have a cardinality and coordinates equal to the corresponding points in the skeleton. Edges are assigned the length along the link points of the corresponding skeletal line segment as an attribute, corrected for digitization effects, leading to a weighted graph structure.
- The longest path in the weighted graph represents the longest skeletal line (Fig. 2d). On this basis, we further distinguish first-order lateral branches, which are connected to the longest path, second order lateral branches, which are connected to first-order lateral branches, and so on. The original positions of the trajectory are projected on the closest point of the longest skeletal line (Fig. 2e). As

a consequence each projection is characterized by three parameters: 1) a length parameter that gives the length along the link points of the longest skeletal line, 2) a parameter that gives the distance between original and projected position, and 3) a parameter that gives the distance of the projected position to the boundary of the binary image of the region. Since the original positions are ordered in a time-sequence, the length parameter also contains information on the direction of movement (forwards or backwards) with respect to the longest skeletal line (Fig. 2f).

Quantification of the Movement Patterns

Features allowing quantification of the movement pattern were derived from the (weighted) graph structure, the movement direction on the longest skeletal line, and the distance between original position and longest skeletal line. The idea was conceived that the longest skeletal line represents the actin filament on which the movement is based. This interpretation leads to three biological criteria that can be used to differentiate in the feature analysis. i) An actin filament is a relatively straight, unbranched protein chain. ii) The polarity of the actin filament dictates the direction of movement. iii) The distance between an actin filament and the center of an attached organelle is maximally equal to r_{org}. Possible displacements of the real actin filament underlying the movement (observations in living plant cells; D.D. Miller and E.S. Pierson, personal communications) are included in the shape of the hypothetical filament, which is derived from a time sequence of the organelle positions. The thickness of actin filaments (5–7 nm) and filament bundles can be neglected compared to the error in the measurement of organelle position and diameter. Programmes for the analyses were written with version 6.07 of SAS (Statistical Analysis System, SAS Institute, Inc., Cary, NC).

Features of the (weighted) graph structure. The graph structure provides a symbolic description of the movement trajectory. The following features were determined for each organelle.

- G1 is the total number of lateral branches of the first order. This feature gives all branch points of the longest path and indicates possible irregularities in the movement pattern.
- G2 is the corrected number of lateral branches. The length of first (and second) order lateral branches has to be $> r_{org}$ to be included in G2. These lateral branches indicate a movement partly without contact with the longest path.
- G3 is the total length of the edges in the longest path. A longer path length indicates a larger likelihood that the path indeed represents an actin filament.
- G4 is the angular deviation. All edges have a start and end vertex and, thus, an orientation denoted by the angle with the *x*-axis. The angular deviation is the difference in angle between the first and last edge in the longest path. A larger deviation indicates a more curved path and a lower likelihood that the path matches a single (straight) actin filament. Angular deviations can not be calculated for graph structures with only one edge (G1=0).

Features of the movement direction along the longest skeletal line. The direction of the longest skeletal line is defined by the direction in which the largest movement distance is covered. Increase or decrease in the length parameter (with respect to longest skeletal line direction) indicates forward or backward directed movement at each position (Fig. 2f). By definition, a displacement was assumed to be real when the region occupied by the organelle at a certain position had nothing in common with the region occupied at the starting position. In practice, the displacement distance then exceeded the size of the organelle diameter.

Features can be determined from the direction of movement at each position and, also, from the preservation of direction. The longer the movement in one direction, the higher the probability that this movement is generated by an actin-myosin interaction. Linear movement is defined as chronologically continuous movement in which the directional progression on the longest skeletal line exceeds a distance equal or larger to the diameter of the organelle. Movement is defined to be non-linear in all other cases. The following features were calculated for each organelle.

- M1 is the fraction of linear movement. The parameter is 1.00 for exclusively forward directed movement and zero for completely non-linear movement.
- M1b is the fraction of linear movement in backward direction. Linear movements in forward and backward direction may indicate movement along a bundle with actin filaments of opposite polarity.
- M2 is the number of stretches with linear and non-linear movement. The value is one if M1=0.00 or M1=1.00. Higher numbers indicate alternations of linear and non-linear movement.
- M3 is the mean distance covered during linear movement. The minimum value is equal to the organelle diameter, except when M1=0.00, then it is zero. The longer the distance of linear movement, the more probable a stable actin-myosin interaction has occurred.
- M4 is the mean endurance time of non-linear movement. This feature is zero if M1=1.00. The longer the time spent in non-linear movement, the smaller the probability of a close interaction between organelle and actin filament.
- M5 is the residual distance of the longest skeletal line. This feature gives the result of the length of the longest skeletal line plus the distance covered in the backward direction subtracted from the distance covered in the forward direction. M5 is zero if all movement in the backward direction is counteracted by movement in the forward direction. However, this is not the case if the organelle starts or ends its movement at a point along the longest skeletal line. Then, M5 gives the distance to the closest extreme point of the longest skeletal line.
- M6 is the number of times that the length of the longest skeletal line is covered. The feature has a value of

one if M1=1.00. A higher value denotes a movement pattern with forward and backward movement.

Features of the distance between original position and longest skeletal line. In comparison to the previous section, features can be determined from the distance between the organelle and the longest skeletal line at each position, but also from the preservation of filament attachment. Generation of movement by actin-myosin interaction is possible only if the organelle stays attached to the actin filament. Consistently filament-attached movement is defined as chronologically continuous movement in which the distances between organelle and longest skeletal line are $<r_{org}$ during more than one second. The movement is non-filament-attached in all other cases. The following features were calculated for each organelle.

- F1 is the fraction of the movement time that the organelle is consistently filament-attached. The feature is 1.00 if the organelle remains attached to the filament during the total duration of the trajectory. A lower value indicates that part of the movement pattern is more than r_{org} removed from the longest skeletal line.
- F2 is mean endurance of consistently filament-attached movement. This feature equals the observation time if F1 is 1.00. The longer the attachment to the filament lasts, the more probable it is that strong the organelle-filament interaction has occurred.

Classification Strategy

Hierarchical classification and continuous ranking was applied to movement patterns according to the strategy in Fig. 3.

- Movement pattern with complete consistently filament-attached movement (F1=1.00) were used directly. Patterns with partly non-filament-attached movement (F1<1.00) or with lateral branches (G2>0) were dissected and re-analyzed to give two or more longest skeletal lines where F1=1.00 for all of them (for reasoning, see discussion on classification strategy). The combined values of the separate parts were used in the following steps.
- The primary classification is based on the presence of actin-myosin generated, and thus linear, movement. Three classes are distinguished based on the fraction of linear movement: exclusively linear (M1=1.00, primary class 1); combined (0.00<M1<1.00, primary class 2); and non-linear (M1=0.00, primary class 3) movement.
- Partly linear movement (primary class 1 and 2) is directed by the polarity of the actin filament. The presence of linear movement in a backward direction (M1b>0.00) distinguishes the secondary class, 1.2 and 2.2, of patterns containing movement on more than one filament. The number of longest skeletal lines in dissected and re-analyzed patterns also defines the secondary class.
- M2, the index for the number of linear and non-linear stretches in one pattern, is the next criterium for classification. It distinguishes the final classes (2.1.2, 2.1.3., and so on) on the alternation in movement type.
- To obtain a ranking order among the organelles present in these classes, G3, the length of the longest skeletal line, was used. Ranking was done for each class separately in descending order.

RESULTS

The above-described method was used to analyze and classify the trajectories of 81 organelles, collected without preferences while moving in the apical 18 µm of a *Nicotiana tabacum* pollen tube. An example showing the first six time lapse positions of an organelle is shown in Figure 1. Various aspects of the derived features and classification strategy are illustrated by ten example trajectories (Fig. 4; see Tables 1–4).

Region-Based Curve Analysis

Most trajectories were adequately described by their graph structures and longest skeletal lines. The graph structure sometimes gave a greatly reduced pattern (examples: Fig. 4b7 and 4b10) or showed a high degree of similarity between the longest skeletal line and the trajectory (example: Fig. 4a6 and 4c6). Incidently, a description which seemed too complex was found (example: Fig. 4b2).

Features of the Weighted Graph Structure

The weighted graph structures of the example movement patterns are presented in Figure 4b1-10 and their feature values in Table 1. Lateral branches were observed in eight of the ten graphs (G1 > 0), but, as the G2 value indicates, only one organelle, 2, showed movement without contact with the longest path. G3 values represented the longest path length. Organelle 7 had the shortest longest path length (G3=0.37 µm), which was just larger than the organelle diameter (0.33 µm). No angular deviation (G4) could be calculated in the cases of organelle 6 and 9 since their graph had only one edge. The large curve in the graph of organelle 5 (G4=119°) indicated a considerable change in direction. The angular deviation of organelle 1 seems too large, but was caused by a short end-edge. None of the graphs in Figure 4b1–10 showed a second-order lateral branch, but an example can be seen in Figure 2d.

In the set of 81 organelles, 16 had a G1 value of 0, and the maximum G1 value was 5. Only seven organelles had a G2 value of 1 or 2, leaving 74 organelles with G2=0. Values for G3 ranged from 0.16 to 11.48 µm. The angular deviation (G4) had values between 1 and 192°. G4 could not be determined in 16 cases. Second-order lateral branches were seen in six graph structures. They all had lengths smaller than r_{org} and, thus, did not represent serious deviations from the first-order lateral branch.

Features of the Movement Direction

Features M1 to M6, derived from the direction of movement on the longest skeletal line, are shown in Table 2 for the ten selected organelles. Three examples showed

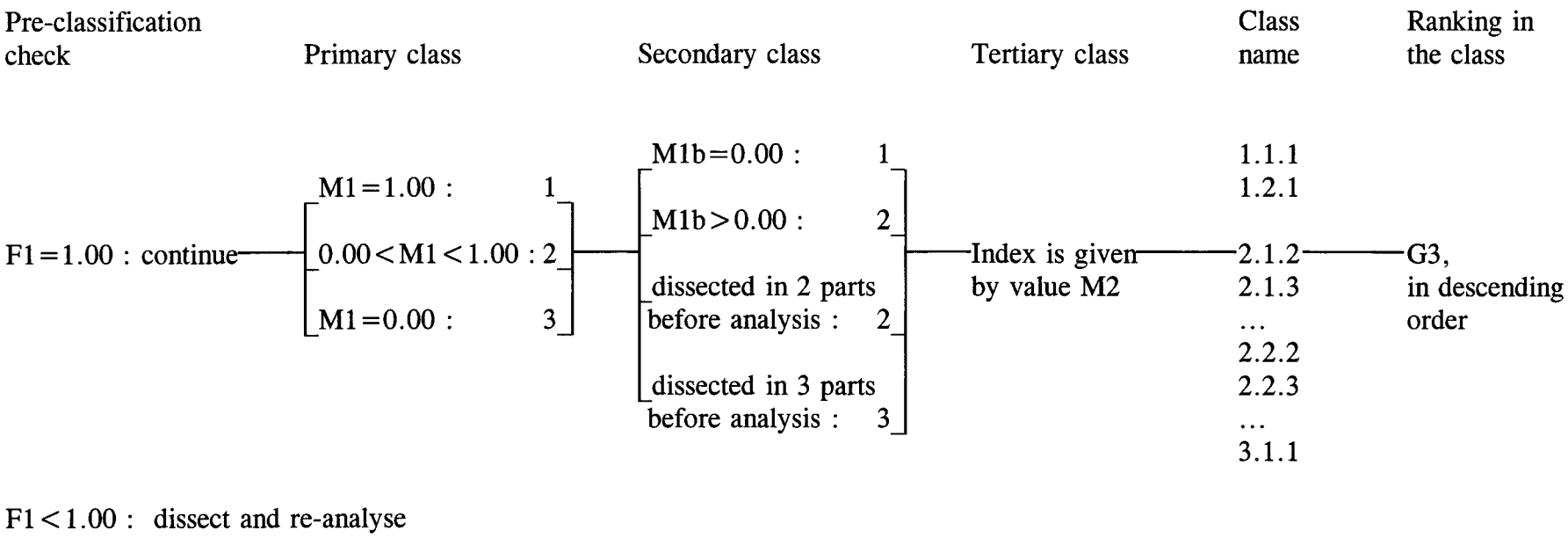

FIG. 3. The classification strategy. The key should be followed from left to right. More details can be found in the text.

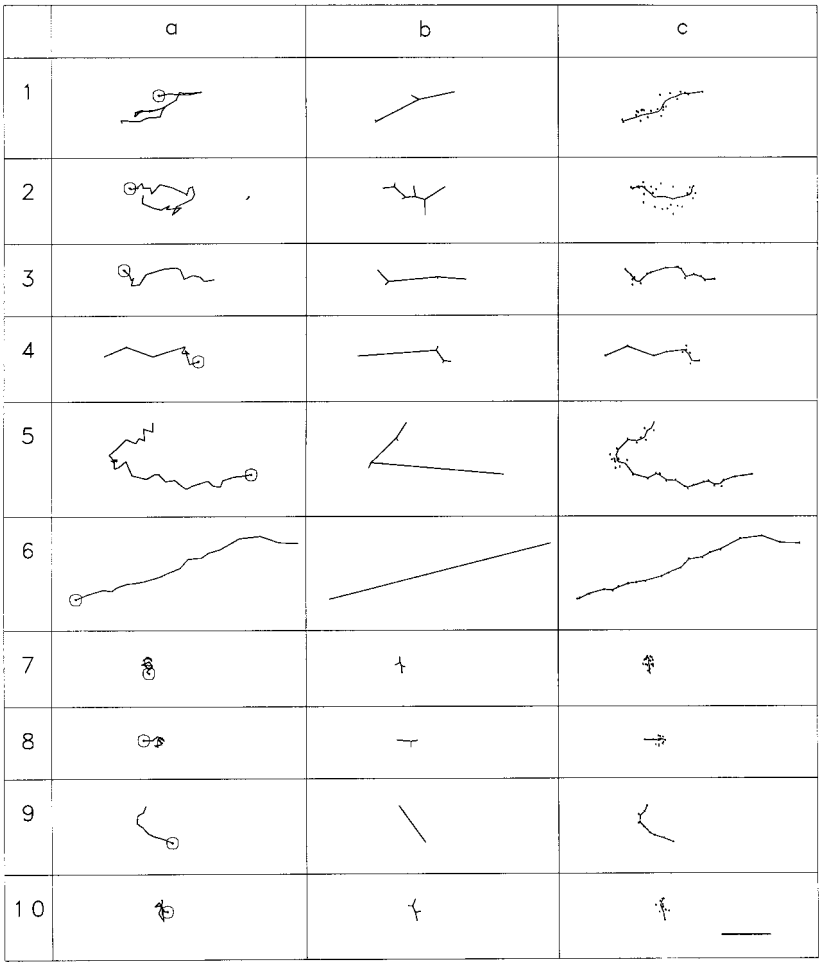

FIG. 4. Ten selected organelle movement patterns. **a1–a10:** The original trajectories. The first position of the movement is indicated by a circle of about the size of the organelle. **b1–b10:** The graph structures. **c1–c10:** The longest skeletal line with the original positions. Scale bar in (c10) = 1 μm for al-c10.

exclusively forward directed movement (M1=1.00: organelle 3, 6, and 9), leading to one movement stretch (M2=1) per pattern and a length of linear movement (M3) equal to G3. Organelle 7 showed total absence of linear movement (M1=0.00), which also led to M2=1 and to an endurance of non-linear movement (M4) equal to the observation time (see also F2). The other examples showed partly linear movement divided over two to six stretches (M2), and with a value for both the (mean) length of linear movement (M3) and the (mean) endurance of non-linear movement (M4). Three organelles (1, 2, and 10) traversed about a third of their distance in linear movement in backward direction (M1b). Note that organelle 8 has a value for M3 equal to G3 although it was partly linear (M1=0.43). Organelle 5 has a non-linear movement stretch of 0.40 s, which is equal to one position. Examples of a return movement (M5) to the beginning (organelles 1 and 10) and from the end (organelles 2 and 8) of the longest skeletal line were seen. M6, ratio of the length along the interconnections between the projected positions and the length of the longest path, provided a measure of reduction.

The presence of small lateral branches could indicate irregularities in the mode of movement and, thus, a relation between the M1, M2, and G1 was anticipated. However, no such relation was found. An organelle (for example, organelle 3) with two small lateral branches (G1=2) could have complete linear movement (M1=1.00, M2=1), while another organelle (for example, organelle 10) with two small lateral branches (G1=2) had four stretches of movement (M2=4) and was partly linear (M1=0.73). Hence, small lateral branches do not indicate irregularities in the mode of movement.

Seventeen of the eighty-one organelles had a M1 value of 1.00, 17 organelles had a value of 0.00, and intermediate fractions were found for 47 organelles. Five organelles had a value for M1b that ranged from 0.26 to 0.38. The maximum value observed for M2 was 9. M3 ranged from 0.35 to 5.79 μm and M4 from 0.40 to 7.60 s. Values for M5 ranged from 0.01 to 1.16 μm and were found for 39 out of

Table 1
*Parameters Derived From the (Weighted) Graph Structure**

Organelle	G1	G2	G3 (μm)	G4 (degrees)
1	2	0	1.88	50
2	4	2	1.55	27
3	2	0	2.18	42
4	2	0	2.17	8
5	2	0	4.42	119
6	0	0	4.96	ND
7	2	0	0.37	1
8	1	0	0.44	9
9	0	0	1.24	ND
10	2	0	0.48	33

*G1, total number of lateral branches of the first order; G2, number of lateral branches with a length $> r_{org}$. G3, total length of the edges in the longest path; G4, angular deviation, difference in angle between the first and last edge of the longest path; ND indicates that a value could not be determined which happens when G1 = 0.

Table 2
*Parameters Derived From the Direction of Movement on the Longest Skeletal Line**

Organelle	M1	M1b	M2	M3 (μm)	M4 (s)	M5 (μm)	M6
1	0.95	0.34	1	0.98	1.20	0.81	2.18
2	0.72	0.36	6	0.77	1.47	1.16	2.07
3	1.00	0	1	2.18	0	0	1.00
4	0.72	0	2	1.74	2.40	0	1.12
5	0.99	0	3	2.24	0.40	0	1.03
6	1.00	0	1	4.96	0	0	1.00
7	0.00	0	1	0	7.20	0	2.97
8	0.43	0	2	0.44	3.60	0.03	2.32
9	1.00	0	1	1.24	0	0	1.00
10	0.73	0.33	4	0.44	1.40	0.19	2.49

*M1, fraction of the linear movement calculated over the distance along the longest skeletal line; M1b, fraction of linear movement in backward direction; M2, number of stretches with linear and non-linear movement; M3, mean distance covered during linear movement; M4, Mean endurance time of non-linear movement; M5, residual distance on the longest skeletal line; M6, number of times that the length of the longest skeletal line was covered.

81 organelles. M6 was 1.00 for the 17 organelles with M1=1.00 and the maximum was 3.07.

Features of the Attachment to the Filament

The movement was not consistently filament-attached for one of the ten example organelles (Table 3, organelle 2). This organelle also had two lateral branches counted in G2. Values of F2 (time spent in consistently filament-attached movement) were equal to the observation time when F1=1.00. No relation was seen between F2 and the fraction of non-filament-attached movement (1-F1).

Seventy-four out of eighty-one organelles had a consistently filament-attached behavior (F1=1.0). Organelles with non-filament-attached movement (F1 < 1.00) always also had lateral branches (G2>0). Feature F1 can thus replace feature G2. The lowest F1 value was 0.56 and its complement (1-F1) is a measure for the magnitude of the non-filament-attached movement. F2 ranged from 2.00 to 23.20 s.

Table 3
*Parameters Derived From the Distance Between Original Position and Longest Skeletal Line**

Organelle	F1	F2 (s)
1	1.00	9.20
2	0.56	3.00
3	1.00	6.80
4	1.00	4.00
5	1.00	14.80
6	1.00	8.00
7	1.00	7.20
8	1.00	5.60
9	1.00	3.60
10	1.00	4.80

*F1, fraction of the movement time that the organelle was consistently filament-attached; F2, mean endurance of consistently filament-attached movement.

Table 4
*Classification of the Organelles in Figure 4 and Tables 1 and 3**

Organelle	F1 = 1.00	Primary class	Secondary class	Tertiary class	G3
6	Yes	1	1	1	4.96
3	Yes	1	1	1	2.18
8	Yes	1	1	1	1.24
4	Yes	2	1	2	2.17
7	Yes	2	1	2	0.44
5	Yes	2	1	3	4.42
9	Yes	2	2	4	0.48
2	No	2	2	7[a]	2.91[a]
1	Yes	2	2	5	1.88
10	Yes	3	1	1	0.37

*The organelles are listed in their final order. Primary class: 1, M1 = 1.00; 2, 0.00 < M1 < 1.00; 3, M1 = 0.00. Secondary class: 1, M1b = 0.00; 2, M1b > 0.00. Tertiary class: index is value of M2. G3, length of the longest skeletal line. The ranking order of G3 was descending.

[a]Value is the total for both parts after separate reanalysis.

Classification

The classification of the ten example organelles is given in Table 4. Except for organelle 2, the values of features M1, M1b, M2, and G3 from Tables 1 and 2 were used to determine the classes. Organelle 2 (F1<1.00) was dissected in two parts and re-analyzed, after which the combined values of both parts were used for the classification. Organelles 3, 6, and 9 belonged to the same class 1.1.1 and were separated by their longest path length. The trajectory drawings of organelles 3 and 4 seem similar in Figure 4a3 and 4a4 but belonged to different primary classes: 1 and 2, respectively. Organelles 7, 8, and 10 all seemed to be examples of Brownian-like movement but in fact, only organelle 7 had no linear movement and belonged to primary class 3. Yet, organelles 8 and 10 were different in their secondary class, because organelle 10 also had linear movement in a backward direction. These two examples show the discriminatory power of the linear

Table 5
*Classes of Movement Patterns of 81 Organelles in the Apical 18 μm of the Tip of a Tobacco Pollen Tube**

Class	N	G3 range (μm)	Description
1.1.1	17	4.96–0.54	Linear movement along one filament
2.1.2	17	7.38–0.35	n stretches of linear and non-linear movement combined on one filament
2.1.3	11	11.48–0.40	
2.1.4	2	1.69–0.84	
2.1.5	3	9.12–0.87	
2.1.7	2	2.76–2.56	
2.1.9	1	3.41[b]	
2.2.3	1 + 1[a]	1.21–1.08	n stretches of linear and non-linear movement combined on two filaments
2.2.4	2	1.30–0.48	
2.2.5	1	1.88[b]	
2.2.6	2[a]	2.15–1.94	
2.2.7	1[a]	2.94[b]	
2.3.4	1[a]	8.65[b]	n stretches of linear and non-linear movement combined on three filaments
3.1.1	17	0.59–0.16	Non-linear movement

*N, number of organelles in each class; G3, length of the longest path; n, value of M2 or tertiary class.
[a]Result after separate re-analysis of parts of the trajectory.
[b]Only one organelle in this class.

movement features M1 and M1b in the classification of organelle movement patterns.

For 74 of the 81 organelles, the classification was straight forward (Table 5). Five of the seven organelles with non-filament-attached movement ($F1<1.00$) were dissected in two or three parts and re-analyzed (see discussion for reasoning). These trajectories are marked by an [a] in Table 5. Two trajectories could not be dissected in a meaningful way and were not classified.

DISCUSSION

Region-Based Curve Analysis

Region-based curve analysis gave good symbolic descriptions of the movement patterns. The merit of this technique is also that an often complex trajectory is simplified to a single line. The sampling time of 0.40 s caused interpolation of the trajectory over large distances for fast moving organelles. Consequently, the shape of the trajectory and the longest skeletal line were similar. A smaller time interval between measured positions would yield more information on the original trajectory and result in a more detailed symbolic description.

Holes in the binary images of the movement regions were removed before skeletization to obtain a single longest path. This could result in a description which seems too complex (see organelle 2). A solution may be obtained by dissecting the trajectory into two or more parts that together enclose the hole and by reconstituting the longest skeletal line of the original trajectory from each longest path.

Reduction of the binary movement regions to a single pixel line sometimes gave a small, almost symmetric furcation at the end of the graph structure. As a standard, the longest edge was included in the longest path which could result in a relatively large angular deviation, as for organelle 1. Alternatively, choosing the edge with the smallest difference in angle with the neighboring edge is recommended, when the difference in length between the edges of the furcation is small.

Detection of curvature in the longest path is an important aspect of the symbolic description. The angular deviation (G4) considers the shape of the curve by looking at its vertices only. Hence, it does not take into account the local shape of the curve. However, organelles with very smooth changes in direction of movement could still make considerable curves that were not detected by G4, since this feature depends on the presence of vertices with a cardinality of 3 or more (see organelle 9).

Pattern Analysis and Data Collection

Under the applied method of data collection, the trajectory start and end points were determined by the visibility of the organelle in the focal plane. The length of the trajectory and the observation time (F2 when $F1=1.00$) are thus chance occurrences and differ among the movement patterns. It follows that the values of features like G3, M2, and M5 are clipped while other features like G1, M3, and M4 are coupled to the trajectory distance or the observation time. Normally, either uniform observation times or lengths would be required to obtain patterns suitable for comparisons. However, organelle movement patterns, taken from the median focal plane of the cylindrical pollen tube, are random samples from the total organelle movement and thus comparable as such. The 81 organelles analyzed in this report were representative for the organelle movement in the tip of a *Nicotiana tabacum* pollen tube.

Does the Longest Skeletal Line Predict the Actin Filament?

The values of some of the features indicate the probability that the initial hypothesis (the longest skeletal line predicts the actin filament along which the movement takes place) is correct. The most compelling requirement is a constant attachment between organelle and actin filament expressed by completely consistent filament-attached movement ($F1=1.00$) and no lateral branches longer than r_{org} ($G2=0$). Seventy-seven of the eighty-one tested organelles matched these criteria. Examination of the trajectories of the other seven organelles led to the suggestion that their movement could be generated by more than one actin filament (see next section for elaboration of this idea).

The next important requirement for actin-myosin generated movement is the presence of movement in one ongoing direction on the filament, expressed by the fraction of linear movement ($M1>0.00$). This requirement was completely fulfilled for 17 organelles ($M1=1.00$), while another 40 organelles had a partly linear pattern ($0.00<M1<1.00$). Among the last 40 organelles, four organelles showed linear movement in two directions, which suggests that their longest skeletal line represents a bundle of filaments with opposite polarity. The probability

of actin-myosin generated movement was proportional to the length of the linear movement (M3). No linear movement (M1=0.00) was detected in the movement patterns of 17 organelles. Thus, it is not likely that their longest skeletal line predicts the actin filament on which the movement was based, if the movement was actin-myosin generated at all.

The shape of the longest skeletal line is also a factor to consider. Fluorescent labeling of actin filaments showed only smooth changes in filament orientation (15,22,24,37). The angular deviations (G4) in the longest skeletal line should conform to these observations. Although recent publications indicated a certain flexibility of bundles of actin filaments in living plant cells (17,30), no quantitative measurements have been done. Assuming that curves in an actin filament can reach up to 90°, values for G4 with more than 90° decreased the probability of filament prediction. Eight out of fifty-seven organelles with linear movement showed such a large curve in their longest path. An explanation for such large angular deviation might be, the organelle jumping onto another nearby filament.

In conclusion, the longest skeletal line has a high probability of predicting the actin filament on which the movement is based if F1=1.00, M1=1.00, and G4≤90° The lowest probability is given by F1<1.00, M1=0.00, and G4>90°.

Classification Strategy

The classification strategy presented in this paper is based on quantitative values extracted from a symbolic morphological description of the movement pattern so that interpretation differences among observers are avoided. In principle, each derived feature, or combination of features can be used to classify the movement patterns. The wide range of features makes it possible to classify and rank even nearly similar movement patterns; the choice depends on the aim. Here, the chosen features (see Fig. 3) indicate the probability that the longest skeletal line is an actin filament. Before classification, the F1 value was examined and trajectories with partly non-filament attached movement (F1<1.00) were isolated. An F1 value of one was obtained for five of the isolated trajectories after they were dissected into two parts on the most extreme *x*-coordinate, and the two parts were re-analyzed separately. This dissection is based on the knowledge that most actin filaments are aligned more or less parallel to the *x*-axis (the long axis of the pollen tube). Examination of the isolated trajectories suggested that the movements in these trajectories could have jumped to a crossing or nearby filament with opposite polarity. Dissection at the most extreme *x*-coordinate provided an objective criterium to increase the number of classifiable organelles.

Primary classes were formed according to M1 which, in simplified terms, indicates whether the movement is vectorial, random, or a combination of both. Secondary classes were made on the basis of the putative number of actin filaments used for movement generation, as appeared from a M1b>0.00 value or from two (three) longest skeletal lines after dissection. Tertiary classes based on the number of linear and non-linear stretches (M2) respond to the logic that a pattern with only one alternation in movement is closer to an exclusively actin-myosin generated movement than a pattern with several alternations. Alterations from linear to non-linear movement could reflect obstructions of the path along the actin filament by other organelles or cytoskeletal elements. A further subdivision in the classification, for instance, using G4>90°or M5>0.00, could be used to highlight other aspects of the mechanism of movement. The presence of direction changes in the path could point to the presence of aligned or crossing actin filaments. For continuous ranking in the tertiary classes, we used the length of the longest skeletal line (G3), following the rational that a longer length indicates a higher probability that the skeletal line predicts an actin filament. Plotting the longest skeletal lines at their position in the cell will give an impression of the organization of the actin filaments.

Primary class 2 matches movement patterns described by Rebhun (27,28) as ''saltatory.'' Our classification further matches the preliminary classification given by Weiss et al. (41) in the following way: primary class 1 matches continuous movement type I and II, secondary class 2.1 matches interrupted movement type I, secondary class 2.2 matches interrupted movement type II, and primary class 3 matches restricted Brownian motion.

Koles et al. (14) and Weiss and co-workers (40,41) proposed a quantitative method to analyze the velocity in their attempts to classify organelle movements based on movement generation type. Their analysis procedure starts off with reconstruction of the underlying microtubule by linear regression. If region-based curve analysis is used to find the underlying filament, their procedure can be used to analyze non-straight movement patterns as well.

Our classification strategy implies a certain order among and within the classes. It is possible to give a rank score to the organelles as a symbolic indication of the probability that the movement is actin-myosin generated. Of course, this indication of the probability is only relevant within the population of analyzed patterns, but comparison of the rank scores could be used to separate sub-populations quantitatively, e.g., in different areas of a pollen tube. Classification of movement patterns can elucidate changes in the cytoplasmic organization when studying cells at various developmental stages (3), under different physiological conditions (34), or after treatment with cytoskeletal inhibitors (29). The method could be integrated in cell viability tests. The presented approach can be applied to other types of moving particles from biological or other sources, such as cell displacements, walking insects, or drifting molecules on metal surfaces.

ACKNOWLEDGMENTS

The authors are indebted to Prof. Dr. W. Url, Dr. I.K. Lichtscheidl, and the Department of Plant Physiology, University of Vienna for the use of their microscope and video equipment, and to Prof. Dr. E. Roubos for the use of

the VIDAS. Dr. D.D. Miller is acknowledged for discussions on myosins and correction of the English text.

LITERATURE CITED

1. Cai G, Moscatelli A, Del Casino C, Cresti M: Cytoplasmic motors and pollen tube growth. Sex Plant Reprod 9:59–54, 1996.
2. de Win AHN: Quantitative Analysis of Organelle Movements in Pollen Tubes. PhD thesis, University Nijmegen, The Netherlands, pp 146, 1997.
3. de Win AHN, Knuiman B, Pierson ES, Geurts H, Kengen HMP, Derksen J: Development and cellular organization of *Pinus sylvestris* pollen tubes. Sex Plant Reprod 9:93–101, 1996.
4. Derksen J, Rutten T, Lichtscheidl IK, de Win AHN, Pierson ES, Rongen G: Quantitative analysis of the distribution of organelles in tobacco pollen tubes: Implications for exocytosis and endocytosis. Protoplasma 188:267–276, 1995.
5. Derksen J, Rutten T, van Amstel A, de Win AHN, Doris F, Steer MW: Regulation of pollen tube growth. Acta Bot Neerl 44:93–119, 1995.
6. Derksen J, Wilms FHA, Pierson ES: The plant cytoskeleton: Its significance in plant development. Acta Bot Neerl 39:1–18, 1990.
7. Dorst L: Pseudo euclidean skeletons. Proceedings of the International Conference on Pattern Recognition, 1986, pp 286–289.
8. Hammer JA: The structure and function of unconventional myosins: A review. J Muscle Res Cell Motil 15:1–10, 1994.
9. Heslop-Harrison J, Heslop-Harrison Y: An analysis of gamete and organelle movement in the pollen tube of *Secale cereale* L. Plant Sci 51:203–213, 1987.
10. Heslop-Harrison J, Heslop-Harrison Y: Organelle movement and fibrillar elements of the cytoskeleton in the angiosperm pollen tube. Sex Plant Reprod 1:16–24, 1988.
11. Iwanami Y: Protoplasmic movement in pollen grains and tubes. Phytomorphology 6:288–295, 1956.
12. Jiang MY, Sheetz MP: Mechanics of myosin motor: Force and step size. BioEssays 16:531–532, 1994.
13. Kohno T, Kohama K, Shimmen T: Studies on myosin of pollen tubes of lily. J Muscle Res Cell Motil 11:357, 1990.
14. Koles KJ, McLeod KD, Smith RS: The determination of the instantaneous velocity of axonally transported organelles from filmed records of their motion. Can J Physiol Pharmacol 60:670–679, 1982.
15. Lancelle SA, Hepler PK: Cytochalasin-induced ultrastructural alterations in *Nicotiana* pollen tubes. Protoplasma 2:65–75, 1988.
16. Lichtscheidl IK, Weiss DG: Visualization of submicroscopic structures in the cytoplasm of *Allium cepa* inner epidermal cells by video-enhanced contrast light microscopy. Eur J Cell Biol 46:376–382, 1988.
17. Liu GQ, Teng XY, Yan LF: Cytoplasmic fibril network of germinated pollen and the movement of cytoplasmic particles. Acta Bot Sin 32:187–190, 1990.
18. Lloyd CW: The plant cytoskeleton. Curr Opin Cell Biol 1:30–35, 1989.
19. Miller DD, Scordilis SP, Hepler PK: Identification and localization of three classes of myosins in pollen tubes of *Lilium longiflorum* and *Nicotiana alata*. J Cell Sci 108:2549–2563, 1995.
20. Miyata H, Bowers B, Korn ED: Plasma membrane association of *Acanthamoeba* Myosin-I. J Cell Biol 109:1519–1528, 1989.
21. Niblack CW, Pibbons PB, Capson DW: Generating skeletons and centerlines from the distance transform. GVGIP: Graphical Models and Image Processing 54:420–437, 1992.
22. Perdue T, Parthasarathy MV: In situ localization of F-actin in pollen tubes. Eur J Cell Biol 39:13–20, 1985.
23. Pierson ES, Cresti M: Cytoskeleton and cytoplasmic organization of pollen and pollen tubes. Int Rev Cytol 140:73–125, 1992.
24. Pierson ES, Derksen J, Traas JA: Organization of microfilaments and microtubules in pollen tubes grown in vitro or in vivo in various angiosperms. Eur J Cell Biol 41:14–18, 1986.
25. Pierson ES, Lichtscheidl IK, Derksen J: Structure and behaviour of organelles in living pollen tubes of *Lilium longiflorum*. J Exp Bot 41:1461–1468, 1990.
26. Pollard TD, Doberstein SK, Zot HG: Myosin-I. Annu Rev Physiol 53:653–681, 1991.
27. Rebhun LI: Studies of early cleavage in the surf clam, *Spisula solidissima*, using methylene blue and toluidine blue as vital stains. Biol Bull 117:518–545, 1959.
28. Rebhun LI: Polarized intracellular particle transport: Saltatory movements and cytoplasmic streaming. Int Rev Cytol 32:93–137, 1972.
29. Salitz A, Schmitz K: Influence of microfilament and microtubule inhibitors applied by immersion and microinjection on the circulation streaming in the staminal hairs of *Tradescantia blossfeldiana*. Protoplasma 153:37–45, 1989.
30. Schindler M: The cell optical displacement assay (CODA): measurements of cytoskeletal tension in living plant cells with a laser optical trap. Methods Cell Biol 49:69–82, 1995.
31. Seagull RW, Falconer MM, Weerdenburg CA: Microfilaments: Dynamic arrays in higher plant cells. J Cell Biol 104:995–1004, 1987.
32. Sheterline P, Sparrow JC: Actin. Protein Profile 1:1–121, 1994.
33. Shimmen T: Characean cells as a tool for studying actomyosin-based motility. Bot Mag Tokyo 101:533–544, 1988.
34. Shimmen T, Yoshida S: Analysis of the temperature dependence of cytoplasmic streaming using tonoplast free cells of Characeae. Protoplasma 176:174–177, 1993.
35. Staiger CJ, Schliwa M: Actin localization and function in higher plants. Protoplasma 141:1–12, 1987.
36. Tang X, Hepler PK, Scordilis SP: Immunochemical and immunocytochemical identification of a myosin heavy chain polypeptide in *Nicotiana* pollen tubes. J Cell Sci 92:569–574, 1989.
37. Tang X, Lancelle SA, Hepler PK: Fluorescence microscopic localization of actin in pollen tubes: comparison of actin antibody and phalloidin staining. Cell Motil Cytoskel 12:216–224, 1989.
38. van Balen R, Smeulders AWM: SCIL_Image: An environment for collaborative use and development of image processing software. Proceedings of the International Conference on Pattern Recognition Jeruzalem. 1994, pp 543–545.
39. Walker RA, Sheetz MP: Cytoplasmic microtubule-associated motors. Annu Rev Biochem 62:429–451, 1993.
40. Weiss DG, Galfe G, Gulden J, Seitz-Tutter D, Langford GM, Struppler A, Weindl A: Motion analysis of intracellular objects: Trajectories with and without visible tracks. In: Biological Motion: Lecture Notes in Biomathematics, Vol. 89. Alt W, Hoffmann G, (eds). Springer-Verlag, Berlin, 1990, pp 95–116.
41. Weiss DG, Keller F, Gulden J, Maile W: Towards a new classification of intracellular particle movements based on quantitative analyses. Cell Motil Cytoskel 6:128–135, 1986.
42. Williamson RE: Organelle movements. Annu Rev Plant Physiol Plant Mol Biol 44:181–202, 1993.
43. Worring M, de Win AHN: Analysis of complex motion patterns using region based curve analysis. Proceedings of the International Conference on Pattern Recognition Vienna, 1996, pp 388–392.
44. Yokota E, McDonald AR, Liu B, Shimmen T, Palevitz BA: Localization of a 170 kDa myosin heavy chain in plant cells. Protoplasma 185:178–187, 1995.